



ELSEVIER

Journal of Chromatography A, 827 (1998) 241–257

JOURNAL OF  
CHROMATOGRAPHY A

# Theoretical analysis of the behavior of an heterogeneously packed chromatographic column

Maureen S. Smith<sup>a,b</sup>, Georges Guiochon<sup>a,b,\*</sup>

<sup>a</sup>Department of Chemistry, The University of Tennessee, Knoxville, TN 37996-1600, USA

<sup>b</sup>Division of Chemical and Analytical Sciences, Oak Ridge National Laboratory, Oak Ridge, TN 37831-6120, USA

## Abstract

The properties of a chromatographic column packed with a nonhomogeneous mixture of two slightly different packing materials are studied by calculating the migration, the broadening, and the shape alteration of a rectangular band moving under nonlinear conditions along such a column. For the sake of simplicity, the column bed is assumed to be an alternate set of coaxial annular columns of the two materials. A two-dimensional implementation of the equilibrium-dispersive model permits the study of problems of this type, requiring two space dimensions for their modeling, such as this nonhomogeneous column with cylindrical symmetry, a nonplanar injection with a cylindrical symmetry, or a cylindrical central injection. The axial and radial profiles of the band inside the column and its elution profiles are calculated. These profiles depend on both the radial and the axial dispersion coefficients and on the relative difference between the separation factor of the two materials. © 1998 Elsevier Science B.V. All rights reserved.

**Keywords:** Band profiles; Column packings; Preparative chromatography

## 1. Introduction

A practical problem encountered in developing new industrial applications of preparative chromatography to separations or purifications in the pharmaceutical industry arises from the fact that the volumes of typical preparative columns are often larger than the average size of the production batch of a dedicated packing material. Obviously, this is not the typical problem in RPLC with C<sub>18</sub> bonded silica materials nor in other modes of chromatography using neat silica, most ion-exchange resins, and many common size-exclusion packing materials, all of which are produced in relatively large batches. However, it is not uncommon to have to select a more esoteric stationary phase to perform a difficult

separation. A typical column, 20 to 30 cm in diameter and 30 cm long contains a volume of 10 to 20 liters. Many batches of custom-designed chemically bonded silica materials are smaller. The result is that several batches of this packing material are prepared successively and the column must be packed with a mixture of these batches.

We know that sophisticated phases tend to be difficult to reproduce. Analysts have complained for ages that specialized columns have poor batch-to-batch reproducibility [1]. Powders are notoriously difficult to mix and homogenize [2,3]. This is a slow process, requiring long operations during which the powder is moved and tumbled. With brittle materials such as porous silica, a significant amount of fine particles may be generated by abrasion. They have to be eliminated in a further step, before the packing of the column. Fines are adverse to good chromato-

\*Corresponding author.

graphic performance because their presence reduces the column permeability and provides a fresh surface area, which is neither deactivated nor bonded to the custom reagent. As a result, insufficient mixing is carried out, in an attempt to avoid the formation of fines.

Then, the column tends to be packed with a nonhomogeneous bed made of regions in which the properties of the packing are slightly different. In practice, it would probably be better not to attempt any mixing at all but to pack successive sections of the bed with the different lots. Proper use of a dynamic axial compression column would allow the achievement of boundaries between the successive lots which would be nearly flat and perpendicular to the column axis. However, this daring procedure can be undertaken only if the problem is identified ahead of time and the packing manufacturer does not attempt any mixing of the different production batches. Barring this, the engineer has to deal with a column bed which is not homogeneous. It is our purpose to attempt to supply information regarding the degree of homogeneity which is required from the packing material in order to lose a minimum of column performance in the separation. For this purpose, we will use a new implementation of the conventional equilibrium-dispersive model of chromatography to cylindrical problems, i.e., to problems in which one of the conditions depends on the radial dimension of the column. Classical models of chromatography assume that the column is radially homogeneous, so that all the phenomena which take place in it depend only on the column length [4]. However, a number of practical problems cannot be studied with these simple models. Because columns are cylindrical tubes, the consequences of the wall effect are a heterogeneous bed which, as a first approximation, has a cylindrical symmetry. We have recently developed a computer program allowing the calculation of numerical solutions of the equilibrium-dispersive model of chromatography in the case of a column with cylindrical symmetry [5–7]. There are now two space dimensions, the column length and its radius. The orientation around the axis is assumed to have no effect.

There are, of course, no reasons for a column packed with a nonhomogeneous mixture of two packing materials to have a cylindrical symmetry. Lumps of lot A will be found in the mix, together

with lumps of lot B and they will fall at random, with mixed regions in between, separated from the lumps by regions in which there is a composition gradient. The three-dimensional chromatographic problem has not been solved yet. Even if it were, we would need reasonably realistic boundary conditions describing the distribution of the two phases inside the column. However, by properly modeling a column of cylindrical symmetry and using the available solution of the two-dimensional chromatographic problem [5–7], we can already obtain some information regarding the degree of homogeneity required for the packed bed.

To satisfy the two conditions, a cylindrical symmetry and a heterogeneous bed, there are two different geometries possible. As suggested above, the two packings can be piled on top of each other, resulting in a simple one-dimensional problem. Its solution will be taken as a reference to determine the losses made by using the alternative solution. The other possibility consists in assuming the column bed to be made of coaxial, annular, cylindrical columns alternately packed with the two packing materials. The problem will be further simplified by assuming a constant area of the different concentric rings and equal amounts of the two materials. Finally, we assume that these two materials have similar physico-chemical properties, only with slight differences in the numerical values of these parameters (e.g., the equilibrium isotherms follow the same model, only with different numerical parameters). The purpose of this paper is to discuss the properties of this cylindrical column.

## 2. Theory

We first recall briefly the fundamental characteristics of the equilibrium-dispersive model [4], then discuss in detail the changes that must be made properly to model the cylindrical, heterogeneous column described in the Introduction [6,7]. The distribution of the bed composition is represented in Fig. 1.

### 2.1. The equilibrium-dispersive model

The equilibrium-dispersive model assumes that mass transfer across the column is instantaneous and

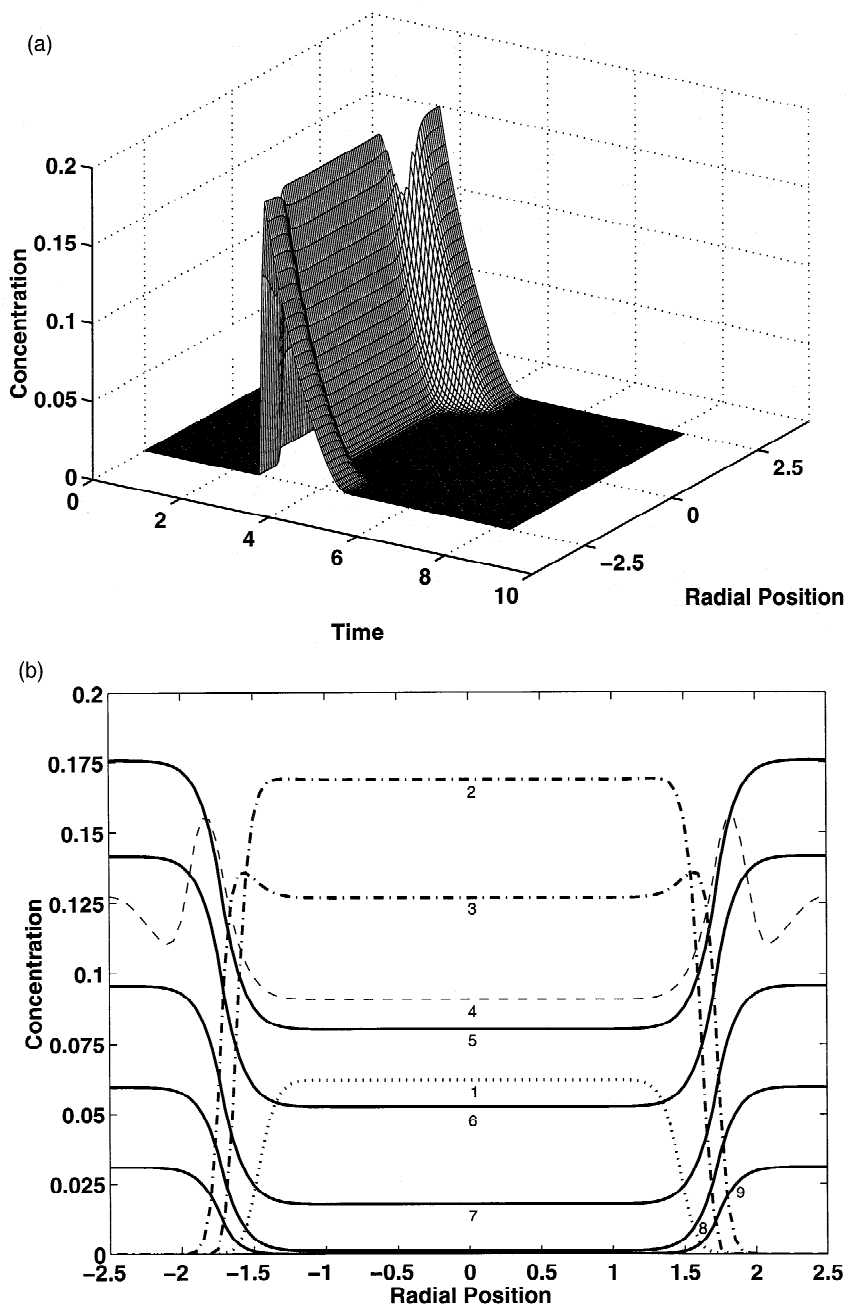


Fig. 1. Elution of a band corresponding to a 10% loading factor on a heterogeneous column made of two concentric annular columns. This is the reference figure for further comparisons. Column length, 15 cm; aspect ratio, 3;  $Pe_a = 2000$ ;  $Pe_r = 10\,000$ . Mobile phase linear velocity,  $u = 0.123$  cm/s.  $t_0 = 121.8$  s. Retention factors:  $k'_1 = 2.25$ ,  $k'_2 = 3.15$ . Isotherm coefficients,  $a_1 = 5.0$ ,  $a_2 = 7.0$ ,  $b = 0.024$ ,  $F = 0.45$ . (a) Three-dimensional representation of the band profile in a  $t, r, C$  space. (b) Plot of the concentration versus the radial position at constant values of the elution time (i.e., sections of the surface in Fig. 1a by planes  $t = \text{const.}$ ). Values of  $t$ : curve 1, 2.19; curve 2, 2.26; curve 3, 2.46; curve 4, 2.66; curve 5, 2.72; curve 6, 2.92; curve 7, 3.25; curve 8, 3.92; curve 9, 4.25. (c) Plots of the concentration versus the elution time,  $t$ , at constant value of  $r$  (i.e., sections of the surface in Fig. 1a by planes  $r = \text{const.}$ ). Values of  $r$ : curve 1, 0.00; curve 2, 1.20; curve 3, 1.70; curve 4, 2.25; curve 5, 2.50. (d) Plot of the radial position,  $r$ , versus the elution time,  $t$ , at constant values of the concentration (i.e., sections of the surface in Fig. 1a by planes  $C = \text{const.}$ ). Values of  $C$ : curve 1, 0.0050; curve 2, 0.025; curve 3, 0.050; curve 4, 0.075; curve 5, 0.100; curve 6, 0.125; curve 7, 0.150. In all figures, the time scale is in min.

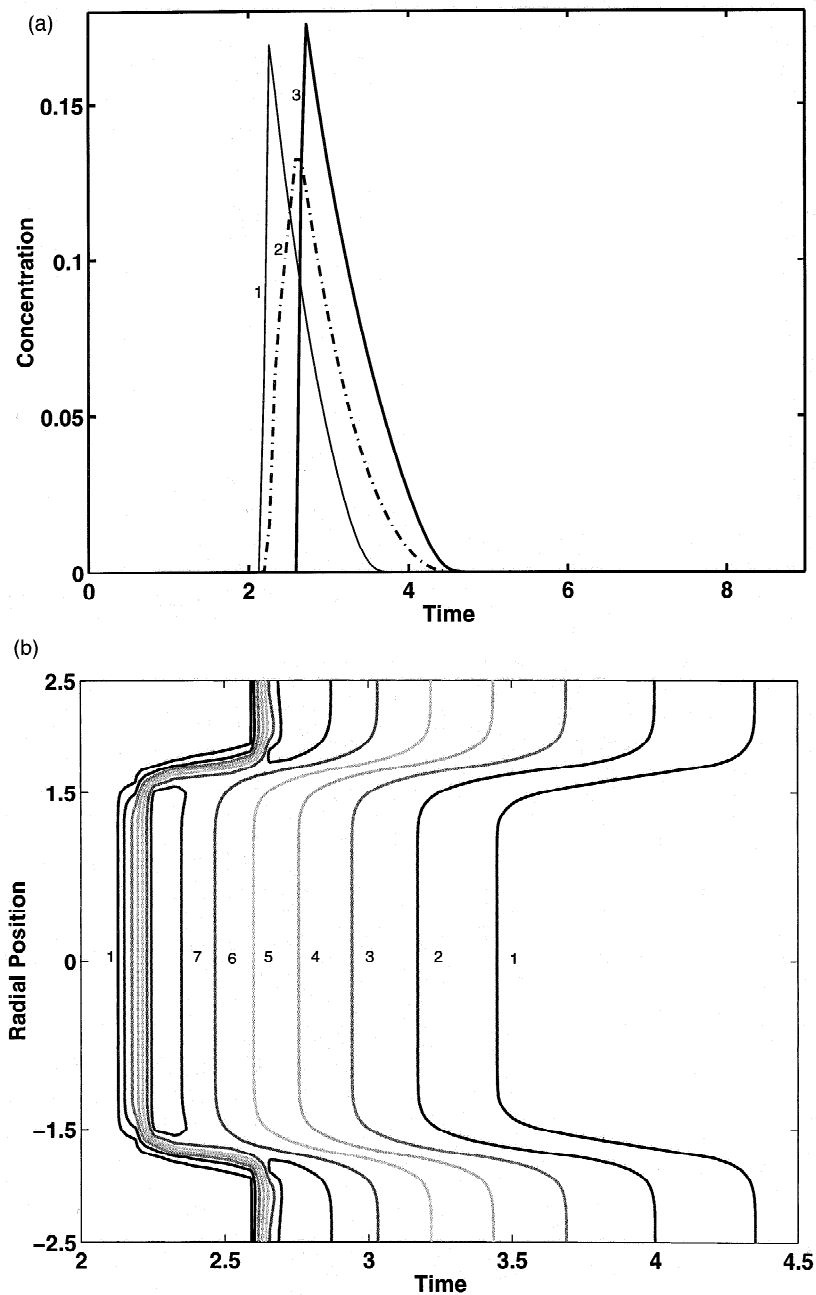


Fig. 1. (continued)

that the mobile and stationary phase at any point in the column are constantly in equilibrium [4]. The actual influence of the mass transfer resistances, which are never negligible, is taken into account by

including it with axial diffusion into an apparent axial dispersion term. Thus, in this model, the apparent axial dispersion coefficient includes contributions for axial diffusion, eddy diffusion and the

mass transfer resistances. We give only a brief summary of the characteristic features of this model, for the sake of comparison. The mass balance equation of the equilibrium-dispersive model for a linear column is written

$$\frac{\partial C}{\partial t} + F \frac{\partial q}{\partial t} + u \frac{\partial C}{\partial z} = D_a \frac{\partial^2 C}{\partial z^2} \quad (1)$$

where  $C$  and  $q$  are the solute concentrations in the mobile and stationary phase, respectively,  $t$  is the time,  $z$  is the distance along the column,  $F$  is the phase ratio ( $F = (1 - \varepsilon)/\varepsilon$ , with  $\varepsilon$ , total column porosity),  $u$  is the mobile phase flow velocity, and  $D_a$  is the apparent dispersion coefficient [4]. The relationship between the apparent dispersion coefficient and the column height equivalent to a theoretical plate (HETP) under linear conditions is given by

$$H_a = \frac{2D_a}{u} \quad (2)$$

Since the equilibrium-dispersive model assumes that the mobile and stationary phase are in equilibrium everywhere in the column, at any time, the concentrations  $q$  and  $C$  in Eq. (1) are related by the isotherm equation. Usually, a Langmuir isotherm model is assumed in theoretical works such as the present one

$$q = \frac{aC}{1 + bC} \quad (3)$$

where  $a$  and  $b$  are numerical coefficients.

The initial and boundary conditions used are those of elution chromatography. Initially, the column is percolated by a stream of pure mobile phase in equilibrium with the stationary phase, with no solute present. A pulse of solute of defined profile, usually a rectangular pulse of height  $C_0$  and width  $t_p$  is injected, beginning at the origin of time.

## 2.2. The mathematical model of a cylindrical column

The simplest deviation from an homogeneous column is an heterogeneous column having a cylindrical symmetry. In this case, the concentration distribution at a given time in a band migrating along the column depends on the position,  $z$ , and the distance,  $r$ , from the column axis. It does not depend

on the azimuthal angle around the column axis. The differential element of the column is a ring of axial thickness  $dz$ , limited by the cylinders of radii  $r$  and  $r + dr$ . In this element, the mass balance is written

$$\frac{\partial C}{\partial t} + F \frac{\partial q}{\partial t} + u \frac{\partial C}{\partial z} = D_a \frac{\partial^2 C}{\partial z^2} + \frac{D_r}{r} \frac{\partial}{\partial r} \left( r \frac{\partial C}{\partial r} \right) \quad (4)$$

where  $D_r$  is the radial dispersion coefficient, related to the radial plate height by

$$H_r = \frac{2D_r}{u} \quad (5)$$

The axial plate height is still related to the apparent axial dispersion coefficient by Eq. (2).

Although, in the general case,  $D_a$  and  $D_r$  could both be functions of the coordinates  $z$  and  $r$  and of the concentration, we assumed in writing Eq. (4) that they are constant.

The presentation of numerical solutions of Eq. (4) and their discussion are greatly simplified if some reduced variables are introduced at this stage. These are the reduced axial position ( $\chi$ ), the reduced radial position ( $\rho$ ), the reduced time ( $\tau$ ), the axial ( $Pe_a$ ) and the radial ( $Pe_r$ ) column Peclet numbers (note that these two Peclet numbers are different from the conventional particle Peclet number or reduced velocity,  $\nu = ud_p/D_m$ ), and the column aspect ratio ( $\Phi$ ) which are defined as follows

$$\chi = \frac{z}{L} \quad (6a)$$

$$\rho = \frac{r}{R} \quad (6b)$$

$$\tau = \frac{ut}{L} \quad (6c)$$

$$Pe_a = \frac{uL}{D_a} = 2 \frac{L}{H_a} \quad (6d)$$

$$Pe_r = \frac{uL}{D_r} = 2 \frac{L}{H_r} \quad (6e)$$

$$\Phi = \frac{L}{R} \quad (6f)$$

where  $L$  is the column length and  $R$  its radius. Combination of Eq. (4) and Eq. 6a–f gives the mass balance equation in reduced coordinates:

$$\frac{\partial C}{\partial \tau} + F \frac{\partial q}{\partial \tau} + \frac{\partial C}{\partial \chi} = \frac{1}{\text{Pe}_a} \frac{\partial^2 C}{\partial \chi^2} + \frac{\Phi}{\text{Pe}_r} \frac{\partial}{\partial \rho} \left( \rho \frac{\partial C}{\partial \rho} \right) \quad (7)$$

There are four parameters in this equation,  $F$ ,  $\text{Pe}_a$ ,  $\text{Pe}_r$ , and  $\Phi$ . In practice, it is extremely difficult, if not impossible, to adjust the first one,  $F$ , which is mostly a property of the packing material and its internal porosity. However,  $F$  depends on the packing density, through the external porosity or fraction of the column volume available to the stream of mobile phase percolating through the column packing. Recent results have shown that the packing density depends somewhat on the stress applied to the column packing during the preparation of the column [8,9]. Still, it does not seem possible to use an adjustable external stress to modify significantly, in a controlled fashion, the column properties. By contrast, the other three parameters are easily adjustable. Note that both  $D_a$  (Eq. (2)) and  $D_r$  (Eq. (5)) are functions of the flow velocity through the corresponding plate height equation. The Peclet number ratio,  $\text{Pe}_a/\text{Pe}_r$ , does not remain constant when this velocity is changed.

### 2.3. Initial and boundary conditions

A description of the column is part of the initial conditions. We assume in this work that the column bed itself is mechanically homogeneous. As in a previous work [6], this allows the assumption that there is no convective transport in the radial direction of the column. This is exact only if the two packing materials differ by their chemistry alone but have the same particle size distribution. Then, there are no radial variations of the packing density, hence the column porosity and its permeability are constant throughout the bed. The radial distribution of the mobile phase velocity is flat. Streamlines remain parallel to the column axis. The only radial variation is that of the retention factor. The two packing materials are arranged in concentric annular columns, each one being homogeneous. For the sake of simplicity, we assume that all sections have the same surface area. We consider a series of columns, the column of rank  $k$  having  $2^k$  concentric rings. The radius of each successive circle is  $r_k = R\sqrt{k/n}$ .

The initial condition of the elution problem is a column under hydrodynamic steady-state, with the mobile and stationary phases in thermodynamic equilibrium, but empty of sample

$$C(x, t = 0) = 0 \quad 0 \leq x \leq L \quad (8)$$

The boundary condition in the axial direction is the injection of a rectangular pulse of sample of concentration  $C_0$  and duration  $t_p$ . This injection extends all across the column. The condition is written as follows

$$C(x = 0, t) = C_0 \quad 0 \leq t \leq t_p \quad (9a)$$

$$C(x = 0, t) = 0 \quad t < 0 \quad t > t_p \quad (9b)$$

Thus, the injected amount is  $n = C_0 t_p F_v$ , where  $F_v$  is the mobile phase flow rate. The loading factor along the column axis is  $L_f = ut_p C_0 / (L(1 - \varepsilon)q_s)$ . The loading factor is the sample size referred to the monolayer capacity of the adsorbent in the column bed.

There are also two boundary conditions in the radial direction. They state that (i) no concentration can penetrate inside the column wall and (ii) the concentration distribution is symmetrical around the column axis, i.e., that the radial gradient of concentration is 0 at the wall (i) and at the column axis (ii). Hence, the concentration gradient is zero along the column wall and along its axis:

$$\frac{\partial C}{\partial \rho} = 0 \quad \text{for } r = R \quad (10a)$$

$$\frac{\partial C}{\partial \rho} = 0 \quad \text{for } r = 0 \quad (10b)$$

The system of equations just described has no analytical solution. Numerical solutions can be calculated using a suitable program [6,7].

### 2.4. Numerical algorithm and calculations

The model described by Eq. (4) and an isotherm model such as Eq. (3) is an extension of the conventional equilibrium-dispersive model (Eq. (1)) to problems with two space-dimensions, e.g., to the case of a column with cylindrical symmetry. It has no analytical solution but it is possible to write simple computational schemes for the calculation of

its numerical solutions, using finite difference algorithms [4].

In the case in which only one space dimension is considered, the forward–backward numerical scheme has, over alternative ones, the advantage of being much faster. In this scheme, there is a simple relationship between the time and space integration increments and the apparent axial dispersion coefficient or the axial HETP of the column. With the forward–backward numerical scheme, for example, the calculation of numerical solutions of the ideal model ( $D_a=0$  in Eq. (1)) should be carried out with increments equal to

$$\delta z = \frac{H_a}{a-1} \quad (11a)$$

$$\delta t = \frac{aH_a}{a-1} \frac{1+k'_0}{u} \quad (11b)$$

where  $a$  is the Courant number of the problem,  $a = (u\delta t / (1+k'_0)\delta z)$ , which must be larger than 1 with this calculation scheme [4]. This calculation method proves to be extremely fast and the solutions obtained are in excellent agreement with those given by more conventional methods [4]. This makes the approach most attractive for the numerical calculation of solutions of Eq. (4), a calculation which is much longer since the problem has now one more space dimension. Thus, a finite difference algorithm, based on the same principles as the forward–backward scheme used with columns having a single space dimension, was developed and programmed. The details of this program are discussed elsewhere [6,7].

Several series of numerical calculations have been done to illustrate the influence of the main parameters, the radial dispersion, characterized by  $Pe_r$ , the difference in retention factors of the two packing materials ( $k'_2/k'_1$ ), and the average distance between the coaxial annular columns of different packings, characterized by their number,  $k$ .

### 3. Results and discussion

The important parameters of the problem are the thicknesses of the annular columns, the relative difference between the retention factors, i.e., the

initial slopes of the isotherms of the compound studied in the two batches of packing material, and the coefficient of radial dispersion. The average value of the retention factor, the column efficiency (i.e., the coefficient of axial dispersion), the column length, and the loading factor have also some influence on the results. We focus our attention on the first three factors, although we give elution profiles for two values of the loading factor, 0.08% (i.e., under linear conditions), and 10% (i.e., under conditions of serious overloading of the stationary phase).

The annular columns are defined as having an area equal to the fraction  $1/n$  of the column cross-section area,  $n$  being the number of annular columns. In order to have the same proportion of the two packing material in the column,  $n$  must be even. We have studied only the cases in which there are 2, 4, and 8 concentric annular cylinders in the column. This assumption does not claim to produce a realistic model of an actual column packed with a mixture of two different batches of a given packing material. It rather attempts to supply a simple procedure for the calculation of the influence of the radial dimension of the packing heterogeneity on the band profile observed at the column outlet. The results will be qualitatively illustrative of the chromatograms which can be observed in the case of columns packed with mixtures of two lots of a packing material, insufficiently homogenized. The dimensionless radii of the annular columns are 0.706 and 1 in the case of two concentric columns, 0.500, 0.706, 0.866, and 1 in the case of four concentric columns, and 0.353, 0.500, 0.612, 0.706, 0.791, 0.866, 0.935, and 1 in the case of eight concentric columns. This last configuration provides the possibility to investigate the contribution of relatively thin veins of one material in the other.

We have studied only the influence of the bed heterogeneity in the radial direction on the profile of the band of one compound. The influence on the resolution of a binary mixture follows in a straightforward fashion, as well as the loss in production rate and recovery yield. We assumed that the coefficients of the equilibrium isotherm, which is given by the Langmuir equation (Eq. (3)), are constant on the average, with  $a=6.0$ ,  $b=0.024$ , and  $F=0.45$ , hence, at infinite dilution,  $k'=2.70$ . We studied the

effect of a large difference between the retention factors of the two materials, with  $k'_1=2.25$  and  $k'_2=3.15$ . Then we considered two moderate differences, with  $k'_1=2.475$  and  $2.61$  and  $k'_2=2.925$  and  $2.79$ , respectively. Finally, we considered two small differences, with  $k'_1=2.655$  and  $2.6775$  and  $k'_2=2.745$  and  $2.7225$ , respectively.

All these calculations were carried out with a 15 cm long column, 5 cm i.d. These column dimensions are typical of the rather fat columns actually used in preparative chromatography. The values of the axial and radial Peclet numbers were 2000 (a 1000 theoretical plate column) and 10 000, respectively. The corresponding ratio  $D_a/D_r=5$  is typical of what was observed in current practice [10–12]. A few more calculations were carried out to illustrate particular points.

### 3.1. Typical band profile

In order to illustrate more clearly the following discussion, we show the changes in band profiles obtained by changing one parameter at a time. Fig. 1, the reference figure for this study, shows the results obtained when  $n=2$  and, for half the packing material in the column (its core), the coefficient  $a$  is 5 and, for the other half (the outer region), it is 7. Accordingly, the retention factors are 2.25 and 3.15. The band profile calculated under these conditions is illustrated in Fig. 1, with Fig. 1a showing a false three-dimensional plot with the concentration along the vertical axis ( $C$ ), the (normalized) retention time ( $\tau=t_R/t_0$ ) along the abscissa axis, and the (normalized) radial position along the ordinate axis ( $\rho=r/R$ ). Fig. 1b–d shows a series of cuts of the band profile in Fig. 1a by the family of planes of equations  $X=\tau=t/t_0=\text{const.}$ ,  $Y=\rho=r/R=\text{const.}$ , and  $Z=C=\text{const.}$ , respectively.

The profile obtained results from a combination of two phenomena. First, as under conventional conditions, the band broadens in the radial direction because of axial dispersion and of overloading. Its axial profile at any radial position, either in the central or in the wall area, corresponds to a conventional langmuirian profile. This is illustrated by the extreme profiles 1 ( $\rho=0$ ) and 5 ( $\rho=1$ ) in Fig. 1c. Second, the band tends to homogenize radially, by radial dispersion. This is illustrated by the profiles in

Fig. 1b and d which are made of two symmetrical, rather steep curves, which are error functions and connect the flat profiles in the two homogeneous regions (see also Fig. 1a). These curves originate from the difference in the migration velocities of the two parts of the band which migrate in regions of the column where the retention is different. This causes a steep concentration gradient relaxed by radial dispersion. The variance of the error function profiles is given by

$$\sigma_r^2 = 2D_r t = 2 \frac{uL}{\text{Pe}_r} \frac{L}{u} = \frac{2L^2}{\text{Pe}_r} \quad (12)$$

With the numerical values selected for the parameters, a value of 2.1 mm is obtained for  $\sigma_r$ , a value quite larger than the one found in Fig. 1b and d. The reason for that is two-fold. First, the radial concentration gradient builds up progressively under the combined influences of the differential migration velocity of the band in the two adjacent regions; second, because of the perturbation due to the formation of a self-sharpening front [4]. The fact that the concentration gradient takes place in a narrower region of space than predicted illustrates how difficult it would be to achieve radial homogeneity. It would take impractically long columns to achieve standard deviations (given by Eq. (12)) of the order of the column diameter (ca. 35 m). The only alternative is to reduce below a few millimeters the scale of the distances over which there are variations of the physico-chemical properties of the stationary phase.

Finally, the elution profile of the column (Fig. 2, curve 1) is derived from the data in Fig. 1a by calculating the cross-section averaged concentration of the compound as a function of time during the elution of the band. These different figures illustrate the considerable distortion of the band arising from a strong degree of heterogeneity of the column bed.

### 3.2. Influence of the main experimental parameters

The influence of the number of coaxial annular columns, i.e., of the thickness of homogeneous regions of packing material inside the column is discussed first. Then, we consider the influence of the extent of the difference between the two packing



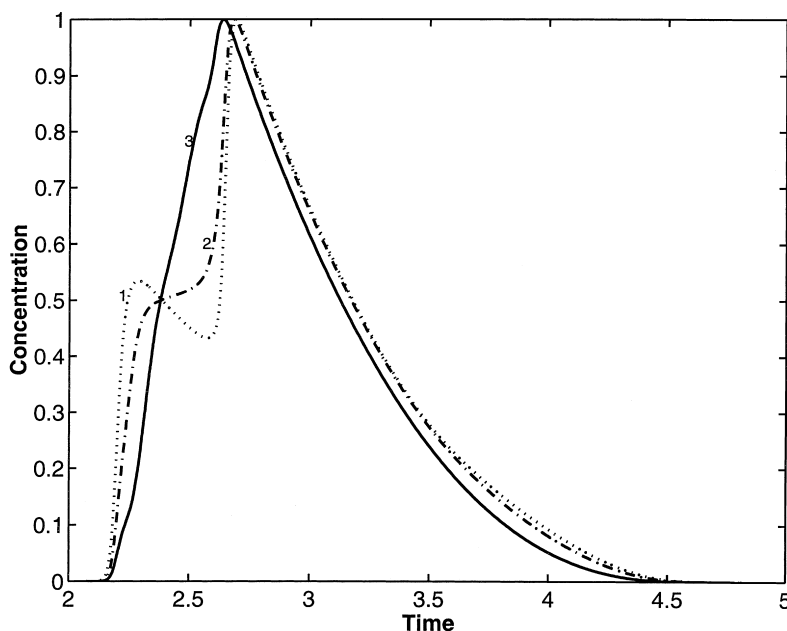


Fig. 2. Elution profiles of a high concentration pulse ( $L_r=0.10$ ) from heterogeneous columns. Retention factors of the two packing materials,  $k'_1=2.25$ ,  $k'_2=3.15$ . The curves are obtained by integration of the effluent composition over the column cross-section. Curve 1: two concentric annular columns (Fig. 1). Curve 2: four concentric annular columns (Fig. 3). Curve 3: eight concentric annular columns (Fig. 4).

materials used to make the column and that of the radial Peclet number and the loading factor.

### 3.2.1. Influence of the number of coaxial columns

The results obtained with four and eight coaxial columns, the other parameters being the same as in Fig. 1, are shown in Figs. 3 and 4, respectively. The global effect of the increase in the number of coaxial columns on the concentration profiles is limited because the central column remains too wide for the corresponding concentration gradient to be significantly relaxed. Nevertheless, a detailed comparison of the band profiles obtained with two, four, and eight columns shows a significant improvement. For example, comparing Fig. 1b, Fig. 3b, and Fig. 4b, which are plots of  $C=f(r)$  at constant time, shows a marked decrease in the amplitude of the concentration fluctuations in the outer region of the band profile. This is obviously due to the decrease in the thickness of the peripheral annular columns when their number increases. The same results would be seen in a comparison (not shown) of the  $r$  versus  $t$  plots at constant concentration (sections of Figs. 1

and 3a, and Fig. 4a) by horizontal planes (cf. Fig. 1d).

The comparison of the elution profiles (Fig. 2, curves 2 for  $n=4$  and 3 for  $n=8$ ) show a rapid change. The elution profile is bimodal for  $n=2$ . It becomes unimodal with a strong frontal hump for  $n=4$ . The hump on the front of the profile disappears for  $n=8$ . Although not yet satisfactory, this last profile could be acceptable under certain conditions.

### 3.2.2. Influence of the relative difference of the retention factors

The same sets of calculations as those whose results have just been described were carried out for lower values of the relative difference between the retention factors of the two lots of the packing materials. Keeping the average value,  $k'=(k'_1+k'_2)/2$  constant and equal to 2.70, values of  $k'_1$  of 2.475, 2.61, 2.655, and 2.6775 have been used, with relative differences,  $(k'_2-k')/k'$  of 16.7, 8.3, 3.3, 1.67, and 0.83%, respectively. The band profiles and the elution profiles were calculated for  $n=2, 4$ , and 8. Part of the results of these calculations are shown below.

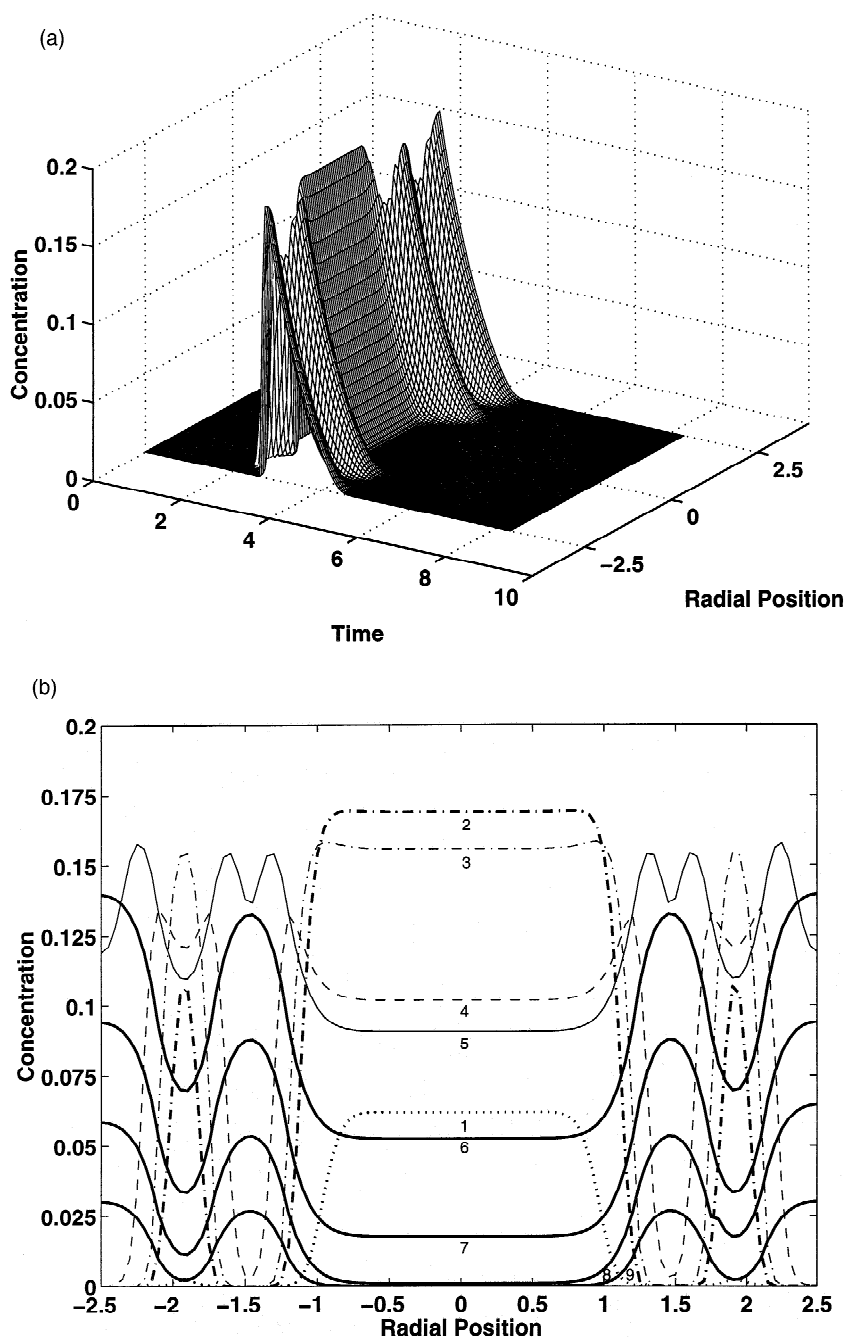


Fig. 3. Elution of a band corresponding to a 10% loading factor on a heterogeneous column made of four concentric annular columns. Retention factors:  $k'_1=2.25$ ,  $k'_2=3.15$ . (a) Three-dimensional representation of the band profile in a  $t, r, C$  space. (b) Plot of the concentration versus the radial position at constant values of the elution time (i.e., sections of the surface in Fig. 3a by planes  $t=\text{const.}$ ). Values of  $t$ : curve 1, 2.19; curve 2, 2.26; curve 3, 2.32; curve 4, 2.59; curve 5, 2.66; curve 6, 2.92; curve 7, 3.25; curve 8, 3.59; curve 9, 3.92.

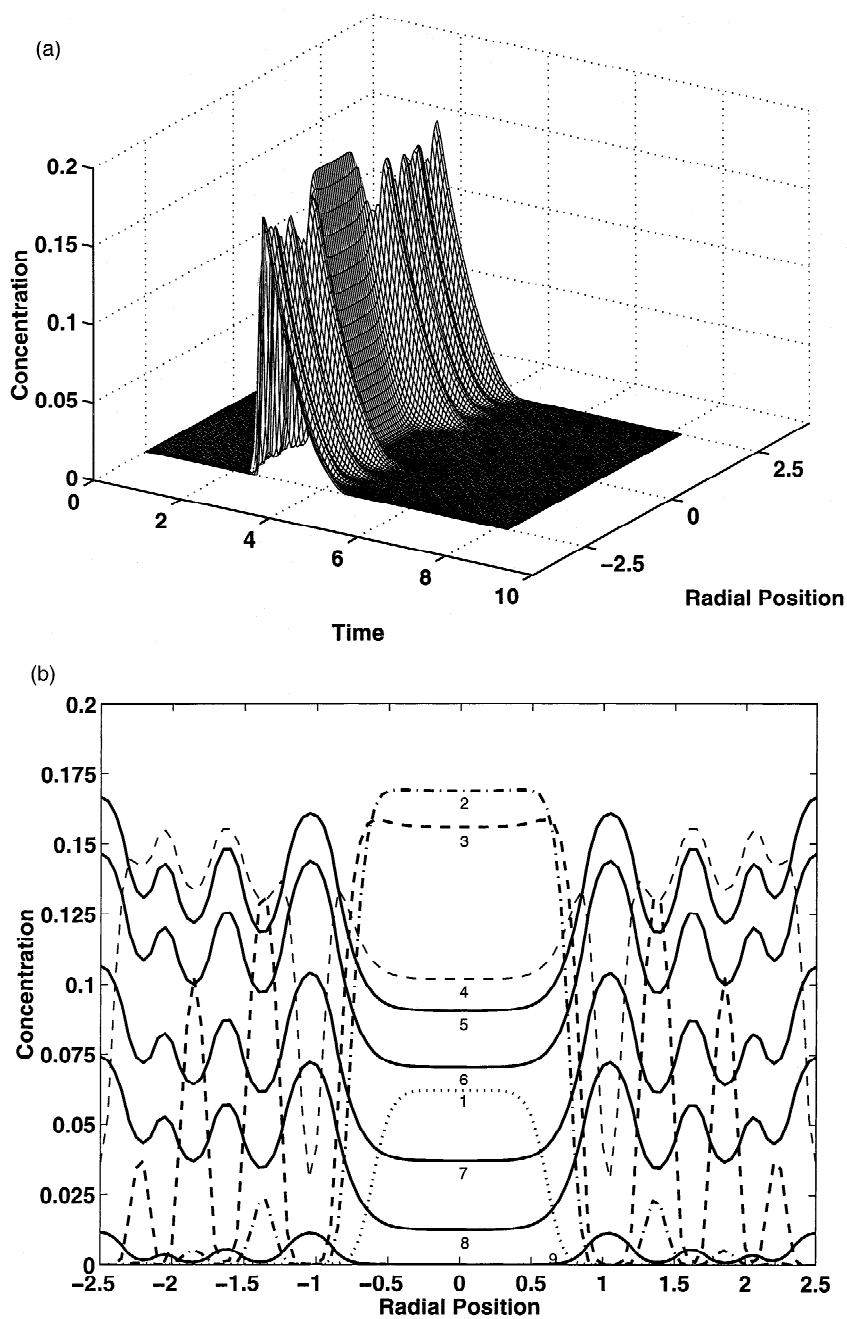


Fig. 4. Elution of a band corresponding to a 10% loading factor on a heterogeneous column made of eight concentric annular columns. Retention factors:  $k'_1=2.25$ ,  $k'_2=3.15$ . (a) Three-dimensional representation of the band profile in a  $t$ ,  $r$ ,  $C$  space. (b) Plot of the concentration versus the radial position at constant values of the elution time (i.e., sections of the surface in Fig. 4a by planes  $t=\text{const.}$ ). Values of  $t$ : curve 1, 2.19; curve 2, 2.26; curve 3, 2.32; curve 4, 2.59; curve 5, 2.66; curve 6, 2.79; curve 7, 3.05; curve 8, 3.32; curve 9, 4.12.

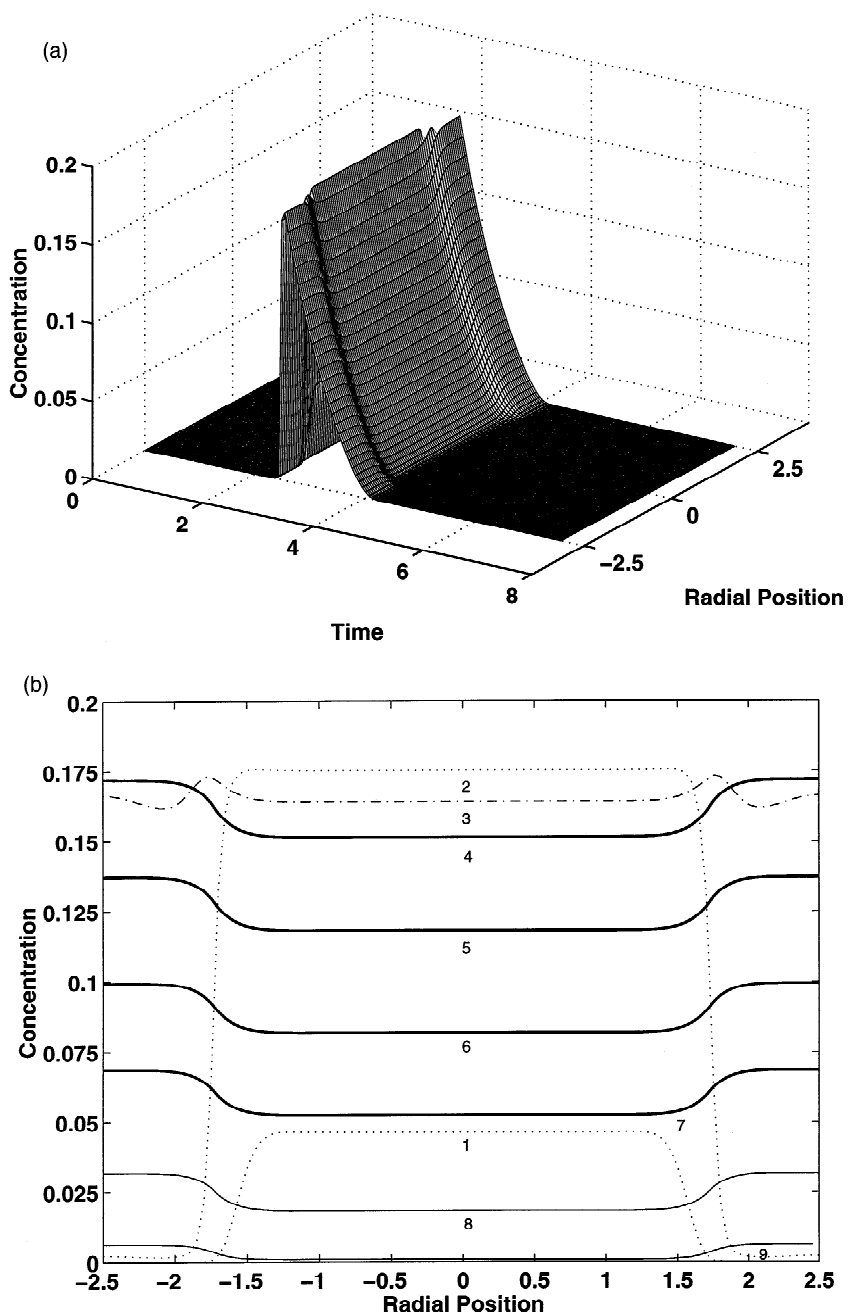


Fig. 5. Elution of a band corresponding to a 10% loading factor on a heterogeneous column made of two concentric annular columns. Retention factors:  $k'_1=2.61$ ,  $k'_2=2.79$ . (a) Three-dimensional representation of the band profile in a  $t$ ,  $r$ ,  $C$  space. (b) Plot of the concentration versus the radial position at constant values of the elution time (i.e., sections of the surface in Fig. 5a by planes  $t=\text{const.}$ ). Values of  $t$ : curve 1, 2.36; curve 2, 2.43; curve 3, 2.49; curve 4, 2.55; curve 5, 2.73; curve 6, 2.97; curve 7, 3.21; curve 8, 3.58; curve 9, 3.94.

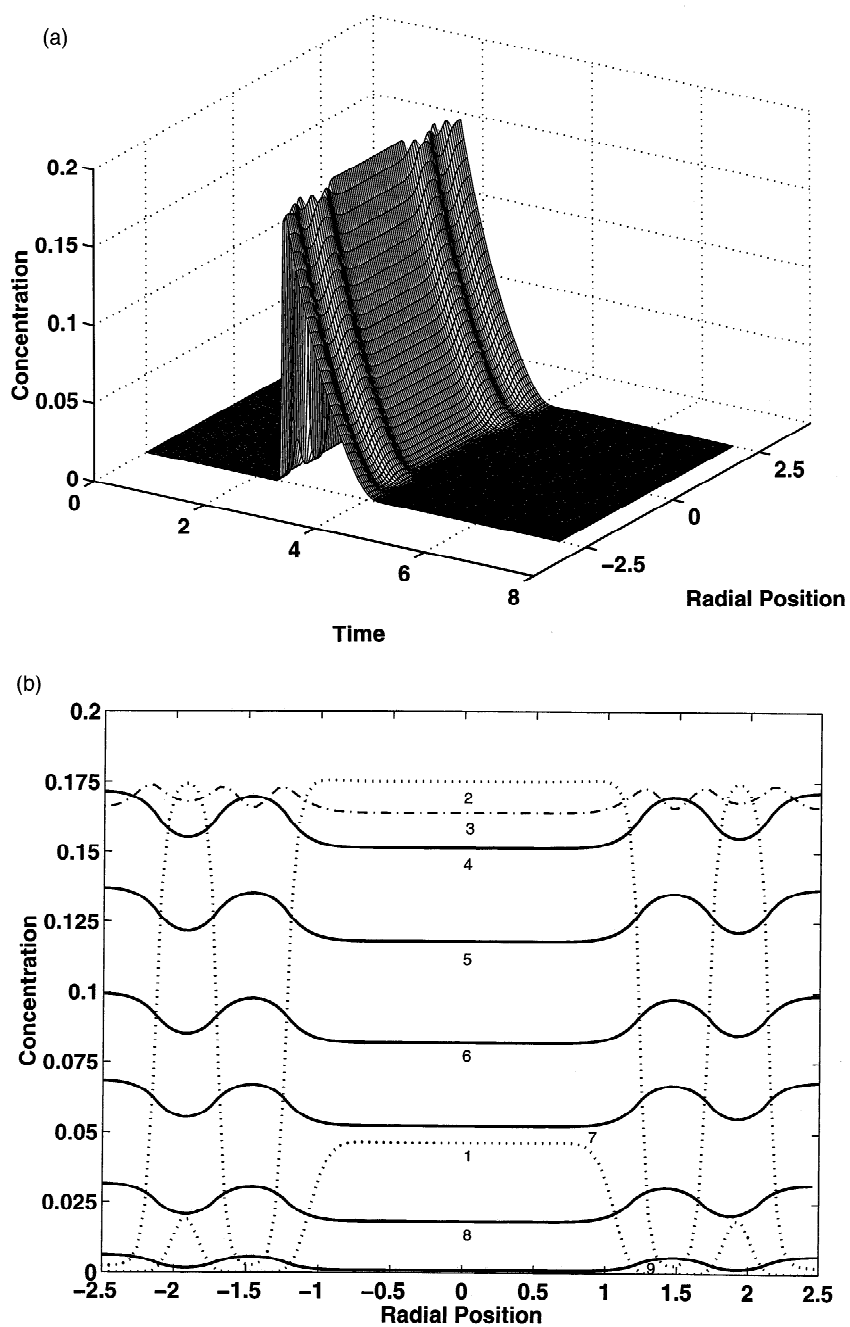


Fig. 6. Elution of a band corresponding to a 10% loading factor on a heterogeneous column made of four concentric annular columns. Retention factors:  $k'_1=2.61$ ,  $k'_2=2.79$ . (a) Three-dimensional representation of the band profile in a  $t$ ,  $r$ ,  $C$  space. (b) Plot of the concentration versus the radial position at constant values of the elution time (i.e., sections of the surface in Fig. 6a by planes  $t=\text{const.}$ ). Values of  $t$ : curve 1, 2.36; curve 2, 2.43; curve 3, 2.49; curve 4, 2.55; curve 5, 2.73; curve 6, 2.97; curve 7, 3.21; curve 8, 3.58; curve 9, 3.94.

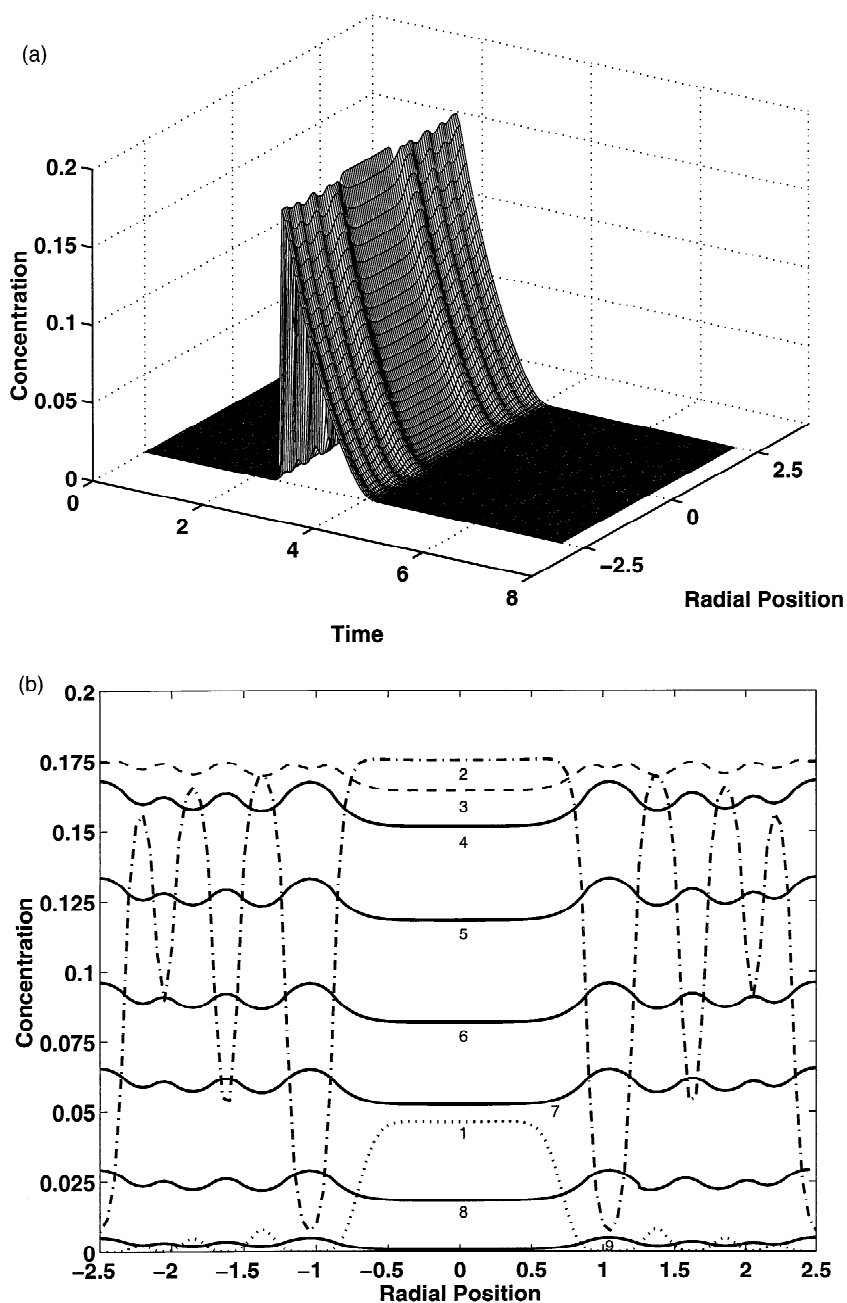


Fig. 7. Elution of a band corresponding to a 10% loading factor on a heterogeneous column made of eight concentric annular columns. Retention factors:  $k'_1=2.61$ ,  $k'_2=2.79$ . (a) Three-dimensional representation of the band profile in a  $t, r, C$  space. (b) Plot of the concentration versus the radial position at constant values of the elution time (i.e., sections of the surface in Fig. 7a by planes  $t=\text{const.}$ ). Values of  $t$ : curve 1, 2.36; curve 2, 2.43; curve 3, 2.49; curve 4, 2.55; curve 5, 2.73; curve 6, 2.97; curve 7, 3.21; curve 8, 3.58; curve 9, 3.94.

Figs. 5–7 show the false three-dimensional band profiles obtained with  $k'_1 = 2.61$ , for  $n = 2, 4$ , and  $8$ , respectively (Figs. 5–7a) and the  $C=f(r)$  sections of these profiles by various planes  $t = \text{const.}$  (Fig. 5b, Fig. 6b, and Fig. 7b). Fig. 8 shows the elution profiles obtained for different values of  $k'_1$  (as many as can be distinguished on the figures) for  $n = 2$  (Fig. 8a),  $n = 4$  (Fig. 8b), and  $n = 8$  (Fig. 8c). Comparison of Figs. 1 and 5, Figs. 3 and 6, and Figs. 4 and 7 shows the considerable influence of the five-fold decrease of the amplitude of the velocity fluctuation,

from 16.7% to 3.3%. The surfaces in Figs. 5 and 6a, and Fig. 7a are not as severely deformed but appear to be corrugated. The radial shift in concentration (Fig. 5b) or the radial oscillations of the concentration (Fig. 6b and Fig. 7b) are considerably reduced, especially in the rear of the band. The effect is much reduced in the front of the band because of the nonlinear behavior at high loading factor and the shock layer at the band front.

When the relative difference between the two retention factors decreases, the elution profile be-

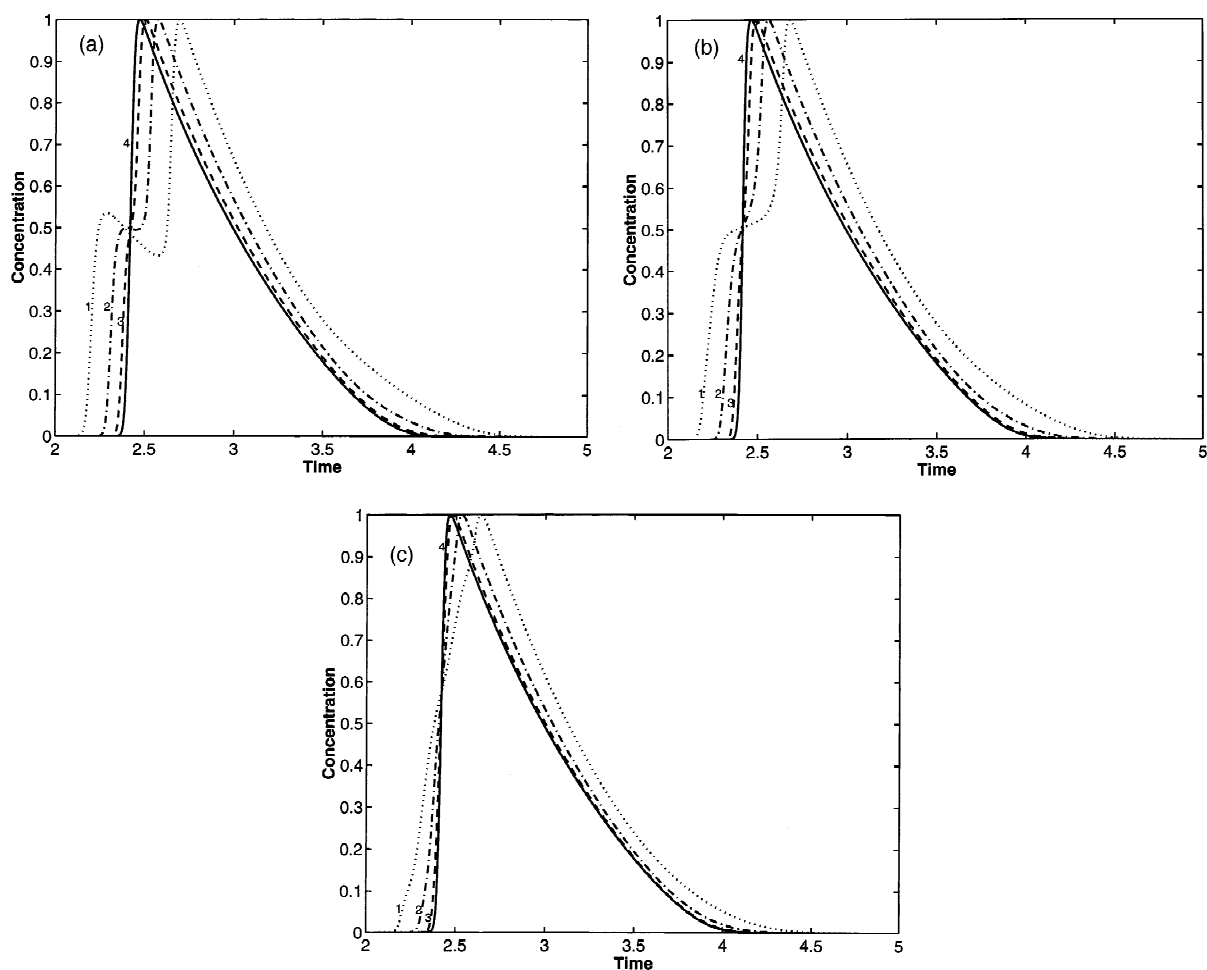


Fig. 8. Elution profiles of a high concentration pulse ( $L_r = 0.10$ ) from heterogeneous columns. Retention factors of the two packing materials: curve 1,  $k'_1 = 2.25$ ,  $k'_2 = 3.15$ ; curve 2,  $k'_1 = 2.475$ ,  $k'_2 = 2.925$ ; curve 3,  $k'_1 = 2.61$ ,  $k'_2 = 2.79$ ; curve 4,  $k'_1 = 2.655$ ,  $k'_2 = 2.745$ . The curve for  $k'_1 = 2.6775$ ,  $k'_2 = 2.7225$  overlay curve 4. The curves are obtained by integration of the effluent composition over the column cross-section. (a) Two concentric annular columns, one for each lot of packing material. (b) Four concentric annular columns, two for each lot of packing material. (c) Eight concentric annular columns, four for each lot of packing material.

comes narrower and tends toward the conventional langmuirian profile obtained with a homogeneous column. The profiles obtained for  $k'_1=2.6775$  cannot be distinguished from those obtained for  $k'_1=k'_2=2.70$ . They cannot be distinguished from those obtained with a column obtained by piling a 7.5 cm long column (length  $L/2$ ) packed with a  $k'_1=2.250$  lot of stationary phase on a 7.5 cm long column packed with a  $k'_1=3.15$  lot of the same material. Because the profiles could not be distinguished, they are not shown.

### 3.3. Radial band broadening during elution under conditions of infinite column diameter

Finally, we show in Fig. 9 the band profiles calculated for the same columns as discussed in the previous section, with a very low loading factor, guaranteeing linear conditions ( $L_f=0.08\%$ ). For a small number of concentric annular columns and a large relative difference of the retention factors, two resolved peaks are observed (Fig. 9a, curves 1 and 2; Fig. 9b, curve 1). Because there is always some

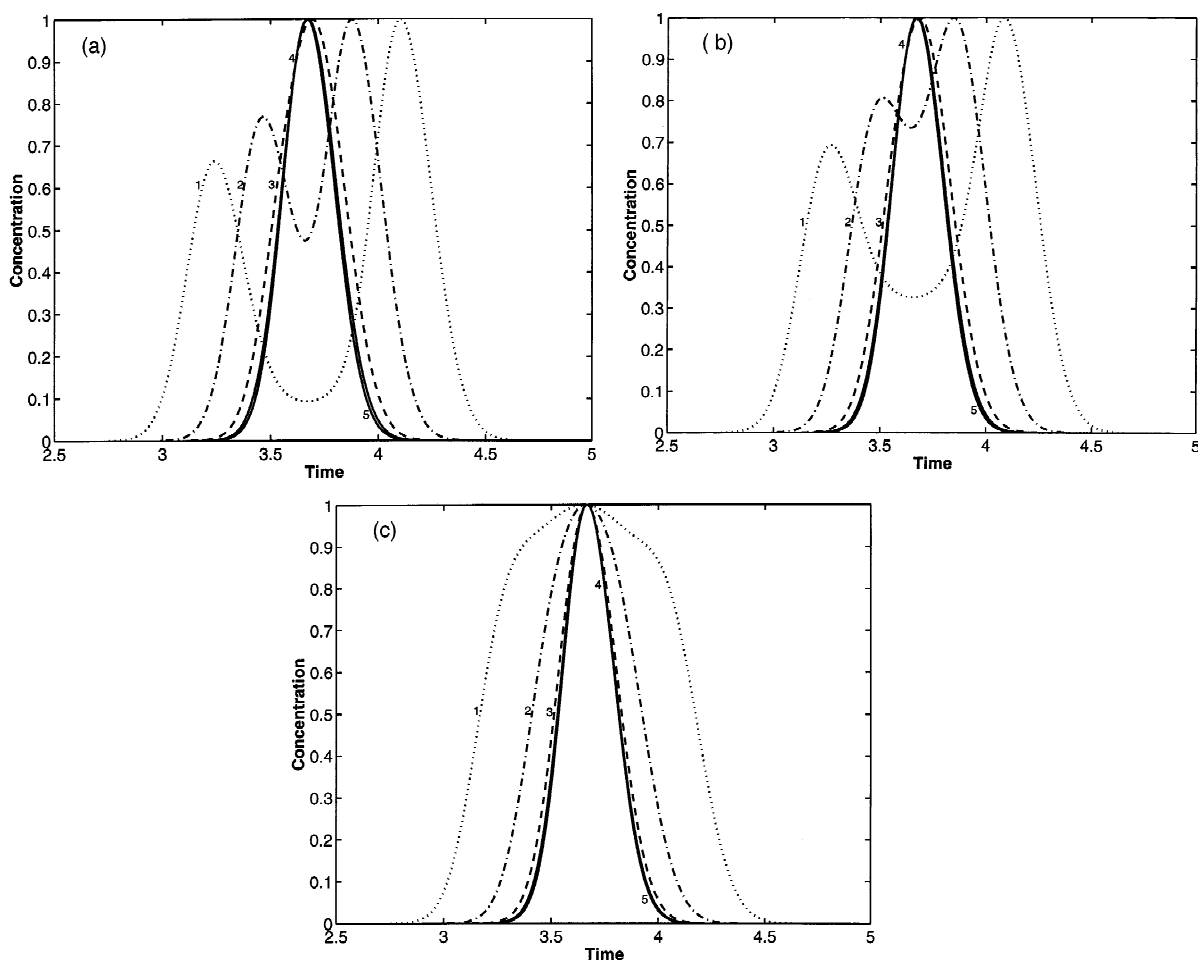


Fig. 9. Elution profiles of a low concentration pulse ( $L_f=0.08\%$ ) from heterogeneous columns. Retention factors of the two packing materials: curve 1,  $k'_1=2.25$ ,  $k'_2=3.15$ ; curve 2,  $k'_1=2.475$ ,  $k'_2=2.925$ ; curve 3,  $k'_1=2.61$ ,  $k'_2=2.79$ ; curve 4,  $k'_1=2.655$ ,  $k'_2=2.745$ ; curve 5,  $k'_1=2.6775$ ,  $k'_2=2.7225$ . The curves are obtained by integration of the effluent composition over the column cross-section. (a) Two concentric annular columns, one for each lot of packing material. (b) Four concentric annular columns, two for each lot of packing material. (c) Eight concentric annular columns, four for each lot of packing material.



extent of radial dispersion, complete resolution could not be observed. However, it is worth noting that for  $Pe_a = 2000$  (i.e.,  $N = 1000$  theoretical plates), at  $k' = 2.70$ , a resolution of 1 is achieved with  $\Delta k'/k' = 0.173$ . This is consistent with the first two curves in Fig. 9a. At lower relative differences in the retention factor and a larger number of columns (i.e., smaller dispersion distances), a unimodal band is recorded. The apparent column efficiency increases rapidly with decreasing relative difference in the retention factors (Fig. 9a–c) and tends toward the expected limit of 1000 theoretical plates.

#### 4. Conclusion

These results confirm that, when two or several lots of a designer packing material must be used to pack a preparative column, the most appropriate course of action, if possible, would be to insist that the different lots be delivered without being mixed. The column should be packed with the different lots, successively. Care should be taken to keep the boundary between each lot flat and perpendicular to the column axis. Then, unless enormous differences between the different lots are experienced, the performance achieved should be the same as with the homogenous mix of the different lots. If this is impossible or if, for any reason, it is preferred to mix the different lots, then this should be done carefully and thoroughly. If there are radial differences between the retention characteristics of the different lots, there should be no significant radial heterogeneity of the column bed over a distance exceeding 1 to 2 mm in the radial direction, unless these heterogeneous regions have also a size of less than 1 cm or so in the axial direction.

#### Acknowledgements

This work has been supported in part by Grant DE-FG05-88ER13859 of the US Department of Energy and by the cooperative agreement between the University of Tennessee and the Oak Ridge National Laboratory. We acknowledge the support of our computational effort by the University of Tennessee Computing Center.

#### References

- [1] B.S. Welinder, T. Kornfelt, H.H. Sørensen, *Anal. Chem.* 67 (1995) 39A.
- [2] H.M. Jaeger, S.R. Nagel, R.P. Behringer, *Rev. Modern Phys.* 68 (1996) 1259.
- [3] K. Muhlbachler, T. Kollmann, A. Seidel-Morgenstern, J. Tomas, G. Guiochon, *J. Chromatogr. A* 818 (1998) 155.
- [4] G. Guiochon, S. Golshan Shirazi, A.M. Katti, *Fundamentals of Preparative and Nonlinear Chromatography*, Academic Press, Boston, MA, 1994.
- [5] T. Yun, G. Guiochon, *J. Chromatogr. A* 734 (1996) 97.
- [6] T. Yun, M. S. Smith, G. Guiochon, *J. Chromatogr. A*, 828 (1998) in press.
- [7] J. Zhang, G. Guiochon, in preparation.
- [8] G. Guiochon, T. Farkas, H. Guan - Sajonz, J.-H. Koh, M. Sarker, B.J. Stanley, T. Yun, *J. Chromatogr. A* 762 (1997) 83.
- [9] B. Stanley, M. Sarker, G. Guiochon, *J. Chromatogr. A* 741 (1996) 175.
- [10] E. Baumeister, U. Klose, K. Albert, E. Bayer, G. Guiochon, *J. Chromatogr. A* 694 (1995) 321.
- [11] U. Tallarek, K. Albert, E. Bayer, G. Guiochon, *AIChE J.* 42 (1996) 3041.
- [12] U. Tallarek, E. Bayer, G. Guiochon, *J. Am. Chem. Soc.* 120 (1998) 1494.